Inspection of templates for imprint lithography

Harald F. Hess,[a] Don Pettibone, David Adler, and Kirk Bertsche
KLA-Tencor 160 Rio Robles, San Jose, California 95134

Kevin J. Nordquist, David P. Mancini, William J. Dauksher, and Douglas J. Resnick
Microelectronic and Physical Sciences Lab, Motorola Labs, Tempe, Arizona 85284

(Received 4 June 2004; accepted 13 September 2004; published 13 December 2004)

Masks of any next generation lithography (NGL), such as imprint lithography, must eventually achieve and maintain the very low defect counts of current production masks. This requires typically fewer than 10 or even no defects over the entire field. We describe an inspection methodology and how it can be applied to the imprint template. Special test patterns etched onto the template enable both a die to die comparison, to find nuisance defects, and also calibration of sensitivity to different types of preprogrammed defects. A state of the art deep ultraviolet photomask inspection system (KLA-Tencor model 526) can detect these rare events with about 70 nm threshold for imprint masks with reflection mode contrast. Initial scans are made at various stages of the imprint process: the newly processed mask, after dicing, and after several imprints. The scans show mostly isolated point defects at a density of ~10–100 per mm^2. This is an encouraging start for a new NGL, and reductions are expected from better processes, equipment, and handling. In the future viable mask inspection at the 45–22 nm node will be very demanding for these 1× masks and will require sensitivities approaching 10–20 nm defect size. To this end, special masks suitable for electron (e)-beam inspection are being made and show good contrast and immunity to e-beam charging. [DOI: 10.1116/1.1813456]

I. INTRODUCTION

Imprint lithography is attracting significant attention as a low cost method for printing nanometer scale geometries. Recently, Sematech has placed imprint lithography on the International Technology Roadmap for Semiconductors (ITRS roadmap) as a potential lithography method at the 32 and 22 nm fabrication nodes. Step and flash imprint lithography (S–FIL) is a particularly attractive method for printing sub-100 nm geometries. Relative to other imprinting processes, S–FIL has the advantage that the template is transparent, thereby facilitating conventional overlay techniques. In addition, the imprint process is performed at low pressures and room temperature, minimizing magnification and distortion errors.[1,2]

However, if imprint lithography is to be considered as a viable method for fabricating high density silicon-based circuits, an infrastructure must be established that is capable of supplying users with high quality 1× templates. It is critical, therefore, that tools are available that can expose,[3] inspect,[4,5] and repair these templates.

S–FIL is a lithographic technique involving many processes and materials such as contact, customized resists, release layers, adhesion, no pellicle protection, etc., all of which threaten to introduce defects. As a first step, inspection with present deep ultraviolet (DUV) reticle inspection tools can help to reproducibly count, benchmark, and identify sources to reduce defect count. We present the methodology, test patterns, and initial results of such an inspection using KLA-Tencor's DUV reticle inspection system for various phases of the imprint process. Iterating on this will hopefully enable imprint lithography to achieve the low density of defects current in production level optical lithography. Today's masks require less than 1–10 printable defects over the 100 cm^2 area. Since a 1× mask has the same requirements over its smaller 6 cm^2 area one might infer that the net tolerable defect density could be higher. In reality the requirements are more demanding.

Since S–FIL is a 1× lithography technology, the template will require essentially no defects larger than 10 nm over the field of the die according to the ITRS 97 for 1× masks at the 45 nm node. This is less than 25% of the design rule. This scaling is comparable to today's requirements for 4× masks in which the 90 nm node is inspected to 72 nm defect size (ITRS 2003 for 4× masks). Many factors like mask error enhancement factors, contrast sensitivity to topography, and imprint rendering will determine the acceptable ratio of defect size to design rule. In any case, the size reduction is so large that DUV optics will no longer suffice and electron (e)-beam inspection will be required.

II. METHODOLOGY

To address these concerns we develop a methodology to inspect the imprint templates with an existing commercial DUV inspection tool and we are exploring how e-beam inspection systems can extend the resolution beyond that of the DUV optical capability.

Two types of S–FIL templates are explored. The first is a pure quartz template. It is fabricated from a standard 6025 quartz plate with a chrome layer and resist. The ZEON Chemical's ZEP520 resist is patterned with a Leica VB6-HR gaussian e-beam writer operating at 100 keV accelerating

[a]Electronic mail: harald.hess@kla.tencor.com

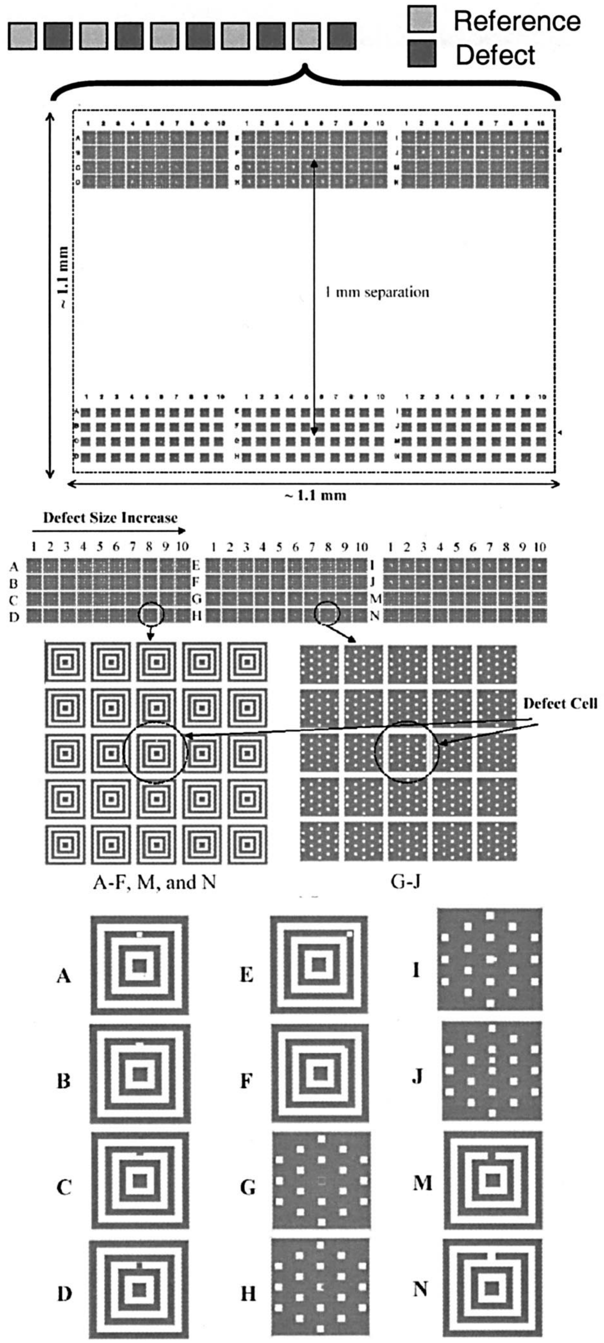

FIG. 1. 4× test pattern arrangement on the imprint template with 400 and 280 nm cells. A similar 1× pattern was printed with 100 and 70 nm patterns.

voltage.[2] The resist image is pattern transferred to the chrome and then the quartz with the chrome and resist removed providing the all quartz template. This template format is suitable for DUV optical inspection.

A different mask is required for e-beam inspection since surface charging from the electrons will prevent generation of the high contrast reproducible images needed for inspection. Such a mask is formed from a quartz substrate that has a transparent conductive oxide layer like indium tin oxide (ITO) capped with another 100 nm of oxide (SiO_2, SiON).

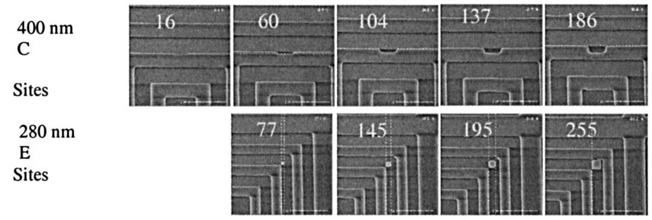

FIG. 2. CD SEM image of programmed defects showing measured size in nanometers. Top row C type edge defects written at 400 nm with sizes 1, 3, 5, 7, 9. Bottom row of E type point defect written at sizes 3, 5, 7, 9.

The process to fabricate this type of template requires the starting 6025 substrate of oxide/ITO/quartz coated with the imaging resist, exposure with e-beam lithography, direct pattern transfer of the resist image into the oxide, and finally removing the resist.[3]

For both cases it is necessary to form specialized test patterns, shown in Fig. 1, that are compatible with the requirements of mask inspection. These patterns and layout were designed with close consultation between KLA-Tencor and Motorola to ensure compatibility with the inspection tool and the S–FIL template requirements. Four different sizes of defect patterns are written: a 4× version with feature sizes designed at 400 and 280 nm intended for compatibility with existing DUV mask inspection and a 1× version with feature sizes designed at 100 and 70 nm patterns for initial e-beam studies. Typically such inspections demand adjacent identical dies. Two high resolution images are formed and subtracted from each other so that any differences highlight the location of a defect. The pattern that defined the die is a 5×5 subarray of either nested squares or a pattern of contact holes. In our case, one of the dies has a sparse array of programmed defects. Various types (A–N) and sizes (1–10) of programmed defects can quantify the sensitivity levels for different patterns. The programmed defects sizes increment from 0% by 10% (A, D, E, G) or 5% (B, C, F, H, I) of the design rule in either just one dimension, edge, defect (B, C, H) or two dimensions for the point and corner defects (A, D, E, F, G, J).

It is important to confirm that the intended defect size is accurately rendered on the template. This enables us to calibrate the sensitivity of the inspection instrument. The critical dimension (CD) scanning electron microscopy (SEM) images in Fig. 2 establish the actual size of the defects. Typically we find that they are within 1% of the design rule.

The template was inspected using a commercial optical reticle inspection tool, the KLA-Tencor RAPID model 526 DUV photomask inspection system. The system operates with 90 nm pixel size. We operated in both transmission and reflection mode at 257 nm wavelength with sensitivity settings that are typical of reticle inspection. Figure 3 shows images taken with the inspection system on a 280 nm pattern in the transmission mode. Both programmed and one nuisance defect can be visually identified. Reflection mode gave a factor of three better contrast than transmission, when the illumination was adjusted to compensate for the low surface reflectivity of these chromeless templates. The optical prop-

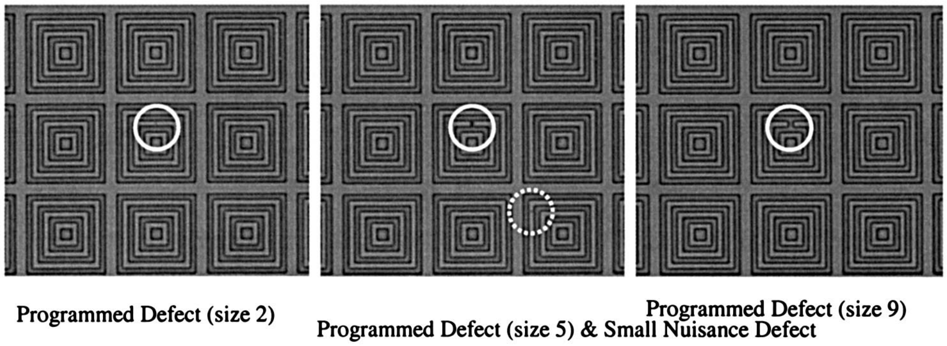

FIG. 3. DUV inspection image of the A type defect written at 280 nm of various sizes and one nuisance defect.

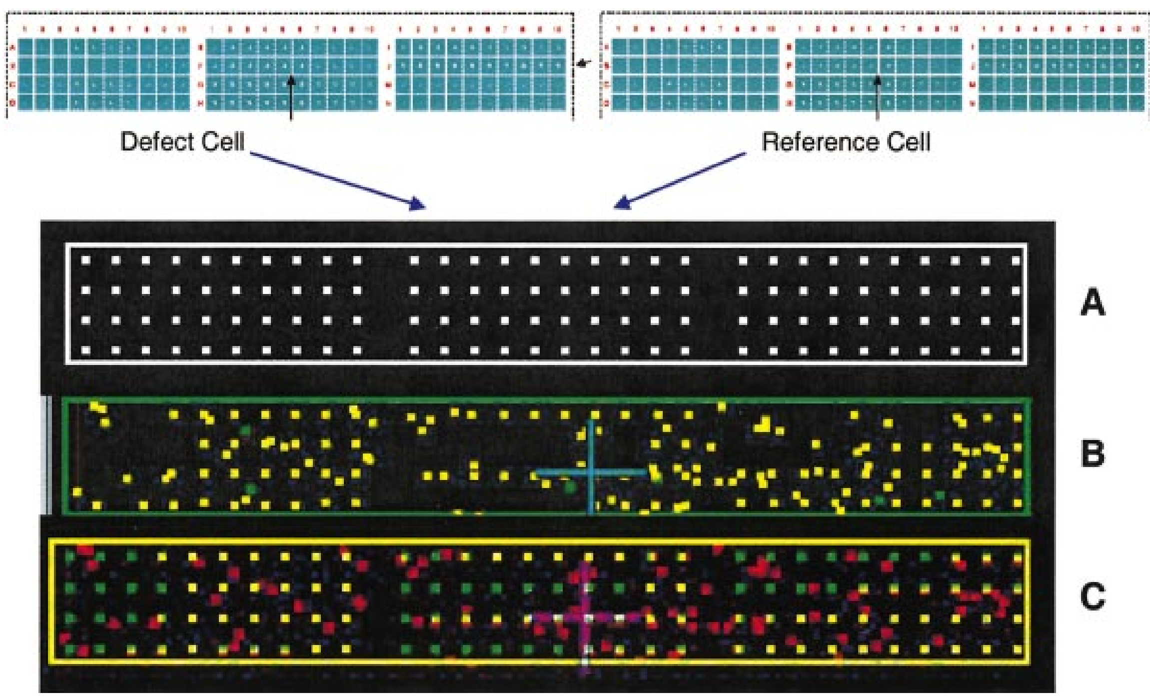

FIG. 4. Reference and programmed defect test pattern are compared for the 400 nm design. In the ideal case with perfect programmed defect sensitivity and no nuisance defects, one would expect the 120 defect array in the pattern labeled (a). (b) shows the actual measured defect distribution for test template No. 2. In (c) the various defects are color coded with yellow for 80 detected programmed defects, green for 40 undetected program defects, and red for the 66 nuisance defects.

erties imprint template can be thought of as a pure phase mask without any chrome and a reduced phase change from the 80 nm relief height in the template. This resulted in better reflective contrast and thus reflection became our preferred method for inspection.

We operate the system in a die to die inspection mode where images of adjacent dies are acquired and compared. Any deviations signal the presence of either a programmed defect or a nuisance defect. The defect count is low enough for proper operation to set some preliminary quantitative numbers. We repeat the inspection six times to certify reproducibility and guard against extraneous error sources. In the ideal case with perfect programmed defect sensitivity and no nuisance defects, one would expect to see the 120 defect

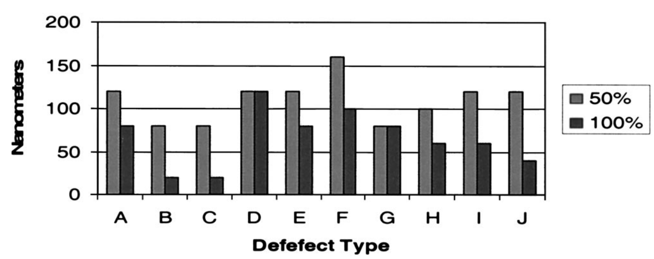

FIG. 5. Bar chart of sensitivity to different defect types as seen with the KAL-Tencor 526 DUV reticle inspection system on template No. 3 with 50% sensitivity (blue) and 100% (purple).

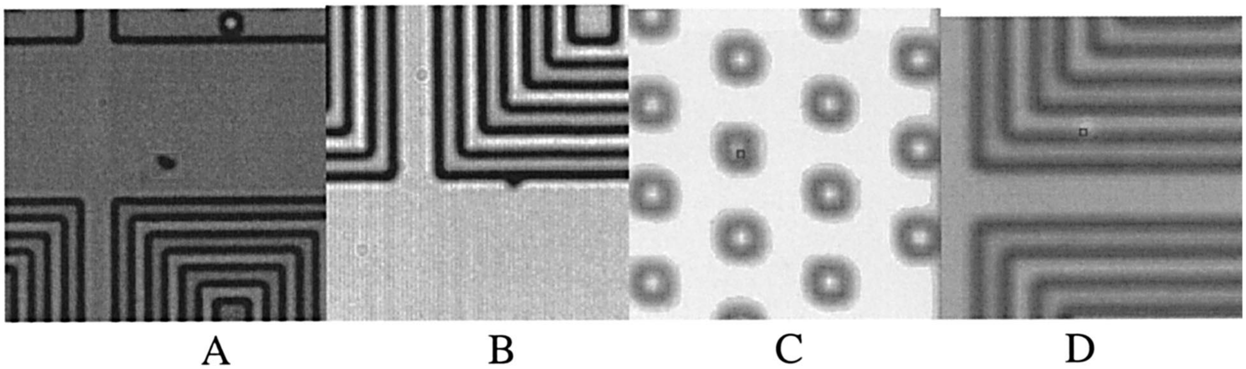

FIG. 6. (a), (b) Various typical nuisance defects, on original plate, (c) programmed defect, and (d) defect after 37 imprints.

array in the pattern labeled Fig. 4(a). Figure 4(b) shows a typical defect map taken after the template was made but before any coating with a release layer. Three types of defects can be identified just by the location information. This is shown by color code in Fig. 4(c). A reduction of sensitivity to about 50% was necessary in order to prevent an overload of nuisance defects. In addition the light calibration parameters are adjusted so that only half of the analog/digital range is used, giving yet a further reduction in sensitivity. The nuisance defects have a density of about 180 defects/mm^2 at these settings. A gauge of sensitivity is given by the number of programmed defects that are detected. In this case 2/3 or 80 of 120 are detected with the system. The remaining 40 either were either below threshold or not printed on the mask.

The sensitivity is quantified for various defect types in Fig. 5 for template No. 3. The light grey shows 50% sensitivity for 400 nm rules. So for example with type A defect the minimum detected size was 3 meaning $3\times10\%=30\%$ of the 400 nm rule or 120 nm. The bar chart in dark grey is for the same template but now tested with 100% sensitivity. Notice the one dimensional edge defects B, C, G are detected with a greater sensitivity approaching 20 nm. The two-dimensional point defects are more challenging to detect and have a higher detection threshold of roughly 80 nm. These are the sensitivity levels used on today's 4× masks.

Further sensitivity improvement can be achieved with a reflective phase contrast rather than pure reflected intensity contrast. This can be controlled by changing the partial coherence of the source illumination. Experience with alternat-

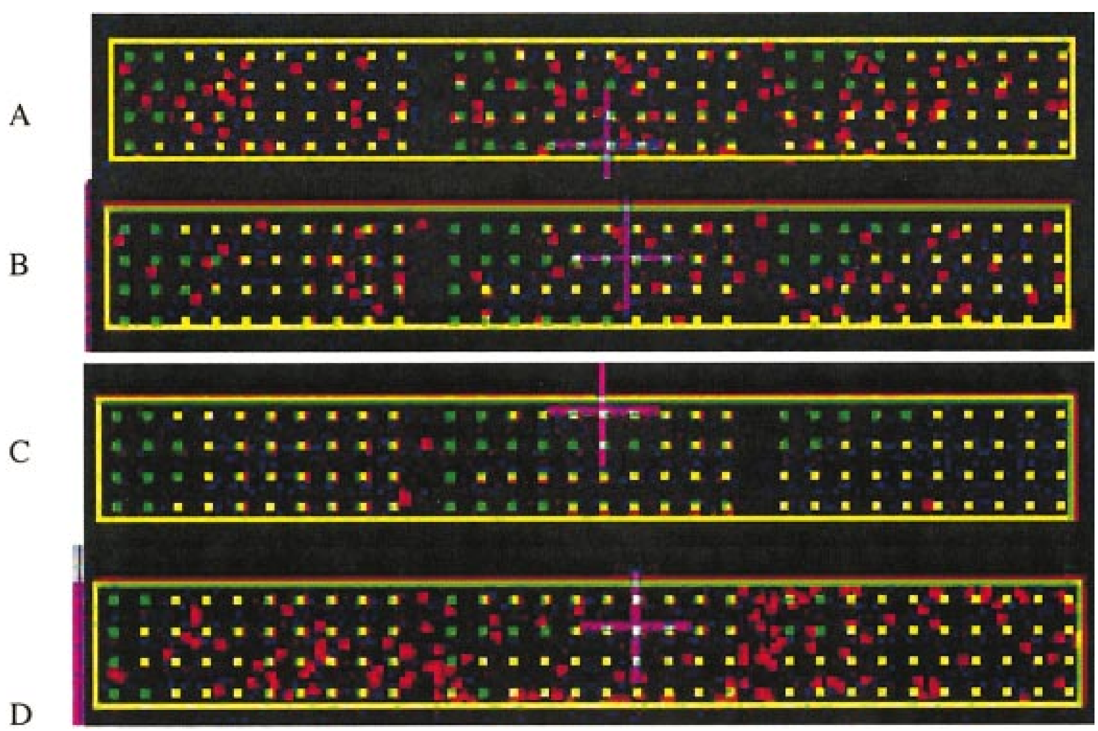

FIG. 7. (a) Defect maps as a function of process steps for template No. 2 before imprints, (b) shows overall defect count reduction after 37 prints, (c) template No. 3 also at 50% sensitivity shows 20× reduced defects, and (d) template with 100% sensitivity.

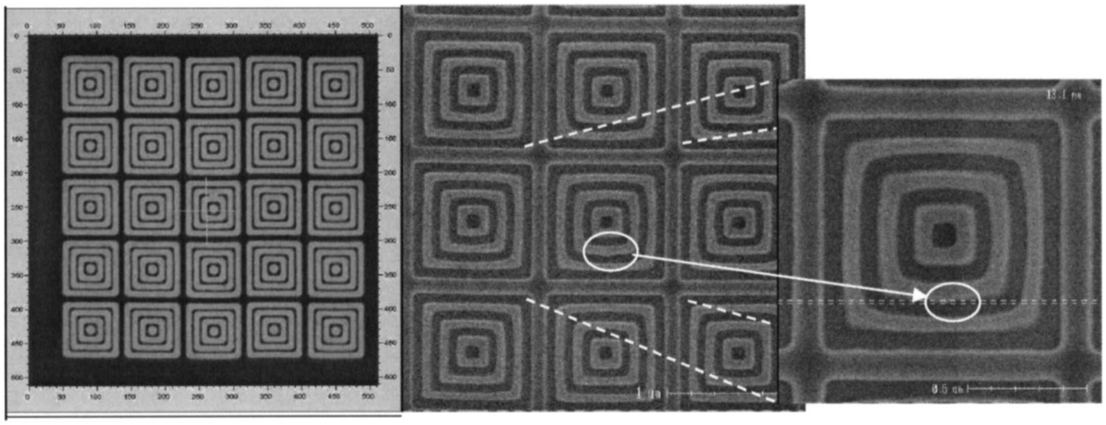

FIG. 8. E-beam inspection picture of 400 nm pattern made on ITO template (left). It shows excellent contrast and no charging effects. A CD SEM image showing 13 nm programmed line edge defect on 70 nm test cell (right).

ing phase shift masks would suggest that this should work also for the S–FIL templates and will be the subject of future investigation.

III. DUV INSPECTION RESULTS

Two very similar templates (Nos. 2 and 3) were inspected. Template No. 2 was taken through various stages of the process and inspected at multiple points to understand the defect contribution of each step. Specifically this template was inspected after patterning the whole 6025 plate, after dicing it, and after 37 more imprints. Care was taken to ensure uniform sensitivity for each inspection by both normalizing settings such as contrast and comparing sensitivity to programmed defects. About 69 nuisance defects are visible over the 0.36 mm^2 inspected area at each stage. Figure 6 shows a sampling of such defects. The dark spots in Figs. 6(a) and 6(b) are typical of the template before any imprinting effort. Figure 6(c) demonstrates successful detection of a H5 (a 100 nm edge protrusion into a contact) programmed defect. Figure 6(d) illustrates a defect after printing.

Typical defect maps before, Fig. 7(a), and after imprinting Fig. 7(b), again give the location of nuisance defects. A visual comparison of these maps show of the 69 original defects, 28 defects were removed, 6 are new and 41 repeat. Multiple sources and types of defects are inferred from the initial processing of the template and from the imprint process. Immediate simple improvements can be made at all steps. An upgraded etching chamber reduced the initial defect count for the next template (No. 3) by a factor of 20 [Fig. 7(c)]. This lower defect count enabled the inspection tool now to operate at 100% sensitivity. Naturally the defect map at this sensitivity level (Fig. 5) is more populated. These are all very preliminary measurements. Better clean room procedures, and newer processes developed by Molecular Imprints Inc.[6] will be implemented and promise a lower defect count in the future.

IV. E-BEAM INSPECTION

Special imprint templates with ITO have recently been made that are consistent with the requirements for e-beam inspection. They have the same patterns as in DUV but the focus will be on the 1× version of the pattern. Good fidelity is achieved and the programmed defects can be calibrated in a CD SEM [Figure 8 (right)]. Such a mask has also been tested on a prototype e-beam inspection system of the KLA-Tencor eS30. The initial images Fig. 8 (left) confirm that these ITO templates are inspectable. This means that two important issues have been resolved: the contrast is excellent and surface charging does not seem to be an issue with the transparent oxide conductors. Present e-beam sensitivity is ~50 nm. Contrast and sensitivity to the full spectrum of nuisance defect types needs to be established next along with inspection feedback on the imprint process. In parallel the sensitivity of future e-beam inspection systems needs to be extended to at least 20 nm to be consistent with 45 nm 1× mask requirements.

V. CONCLUSIONS

A methodology has been established for doing DUV based mask inspection and some initial imprint templates have been inspected. This will be valuable in the interim to guide process development toward achieving low level defect count. A related methodology is being established for e-beam inspection on the smaller patterns and specialized templates.

ACKNOWLEDGMENTS

The authors are particularly appreciative of the efforts of Motorola Lab's Microelectronics and Physical Sciences Laboratory for fabrication of the S–FIL templates and of the suggestions of S. V. Sreenivasan. This work has been funded in part by DARPA fluids Contract No. N66001-02-C-8011.

[1]M. Colburn *et al.*, Proc. SPIE **3676**, 171 (1999).
[2]T. C. Bailey *et al.*, Microelectron. Eng. **61/62**, 461 (2002).

[3]W. J. Dauksher, D. Mancini, K. J. Nordquist, D. J. Resnick, P. Hudek, D. Beyer, and O. Fortagne, presented at MNE 2003 (to be published in Microelectron. Eng.).
[4]D. Pettibone and S. Stokowski, J. Vac. Sci. Technol. B, these proceedings.
[5]W. H. Broadbent *et al.*, Proc. SPIE **5256**, 474 (2003).
[6]S. V. Sreenivasen (private communication).